Proceedings World Geothermal Congress 2020+1
Reykjavik, Iceland, April - October 2021

Geochemical Study of Hanle Geothermal Field, Djibouti

Daher Ali Hassan[a] and Daisuke Fukuda[b]

[a]Djiboutian Development Office of Geothermal Energy (ODDEG)

[b]JMC Geothermal Engineering Co., Ltd.

daherali12@hotmail.com and fukuda@geothermal.co.jp

Keywords: Hanle, Hydrothermal, Aquifer, Geothermometer.

ABSTRACT

The Republic of Djibouti is located in East Africa, in the Great Rift Valley and at the Afar Triple Junction. From a geological point of view, the Hanle lava plateau is composed of basaltic lava layers called the Afar Stratoid Series. Faults or fractured systems were formed in the NW-SE direction in the plateau. Hydrothermal activities are found as fumaroles with temperatures higher than 98°C and a hot spring. Using the chemical compositions of the fumaroles and hot spring, the reservoir temperature was estimated to be 180°C–260°C based on gas geothermometers. Also, the temperature of the hot spring aquifer was estimated to be 125°C based on a solute geothermometer. The major solute components of the hot spring suggest that the spring water is created by mixing of groundwater and heated fossil seawater, or dissolution of evaporate by heated groundwater. Results from geochemical, geological and geophysical studies indicate that a geothermal reservoir lies below the central area of the Hanle lava plateau. In that area, geothermal steam discharges most vigorously at Garabbayis and Goros. These zones can be a prospect for subsequent exploration including test drilling.

1. INTRODUCTION

The Republic of Djibouti is located on the East Africa rift between Somalia and Ethiopia, and it has a 23,000 km^2 surface area. The region located in the south-central part of Djibouti Republic is encountering rapid development, notably due to the intense road traffic on N9, the road linking Djibouti to Addis Ababa. The area is relatively populated and the Hanle plain, which is in the area, is relatively fertile. The development of the area is however delayed by a lack of electricity, as the region has no local energy resources. Dikhil, which is a major town in the area, is presently supplied with electricity by a small diesel plant, being located away from the electric line interconnecting Djibouti and Ethiopia (Figure 1).

Figure. 1: Map of the south-eastern part of Djibouti Republic with the location of the site proposed for geothermal exploration.

In the survey, samples were collected from fumaroles (gas or steam condensate), a hot spring, and water wells (groundwater) in January and September 2016. The samples were analyzed for chemical and stable isotopic composition in Japan. The results of the analysis were interpreted with geochemical techniques to explain the origin of the fumarolic gas and hot spring water, and to estimate the geothermal reservoir temperature.

This geochemical study will be composed as follows: firstly, the sampling methodologies and analytical procedures will be detailed and then the results and, secondly, discussions of these analyses will be discussed.

2. METHODOLOGY

Fumarolic gas was sampled at Garabbayis, Garabbayis North, Adha'amo, Goros, Dimbil, Dirdir and Lafofili, and steam condensate was taken at Garabbayis. A hot spring was found and surveyed only for Kori. Groundwater was sampled from four water wells and sampling locations are shown in Figure 2.

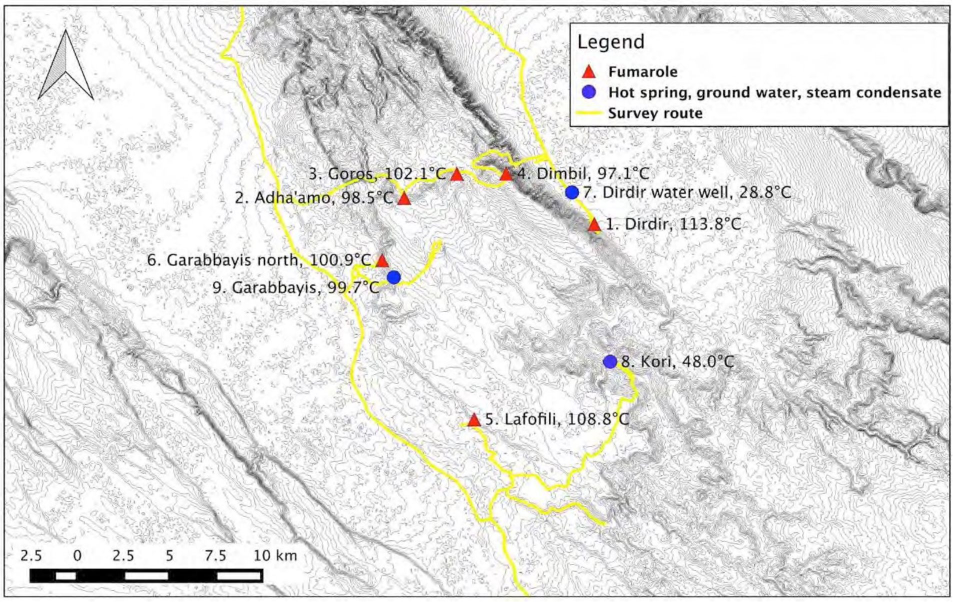

Figure 2: Sampling location map of the geochemical survey in 2016.

2.1 Gas Sampling Method

The method of fumarolic gas sampling is shown in Figure 3. Fumarolic gas sampling is done by the following method: 1) cover the area of fumarolic gas ejection by a funnel that is connected to a gas burette with a rubber tube, 2) collect the fumarolic gas into the gas burette which was filled with a potassium hydroxide solution (5 mol/L) in order to absorb CO_2 and H_2S from the fumarolic gas, 3) collect 8 ml of residual gas (R gas) that is not absorbed by the potassium hydroxide solution.

After cooling the liquid (alkali condensate) inside the gas burette until its temperature equals the outside air temperature, read the volumes of R gas and the alkali condensate. The R gas is transferred into a gas collector. Alkali condensate was transferred into two polyethylene bottles for H_2S and CO_2 separately. Cadmium acetate solution is added to sample for H_2S analysis in order to fix H_2S as the cadmium sulphide in the solution.

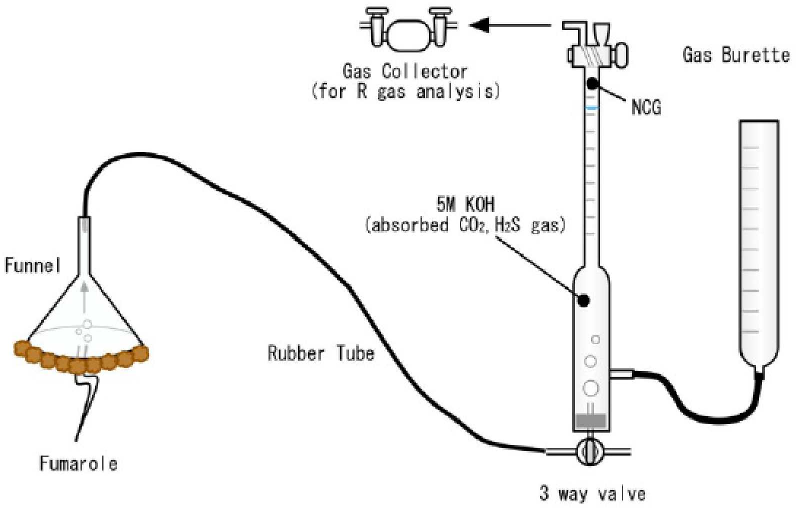

Figure 3: Method used for collecting fumarolic gas (gas burette).

The sample for He and Ne isotope analysis was collected by introducing fumarolic gas into a gas collector directly. Samples of hot spring water, well water and lake water were collected in polyethylene bottles. For some analytical component, pre-treatment was conducted in order to prevent concentration changes before analysis.

2.2 Water Sampling

Samples were taken directly from the source without filtration or cooling. The hot spring and the water well were taken in 4 bottles for analysis of major elements such as Cl, SO_4, Mg, Na, K, Ca, and isotopes.

2.3 Analytical Methods

Analysis of the water samples (hot spring, well water and lake water) and fumarolic gas samples collected in this study was performed by the methods shown in Table 1.

Table 1: Chemical analysis methods.

Analysis items	Pre-Treatment Method	Analysis Method	Detection Method or Accuracy	Analysis standard
Water Samples				
pH	No-pre-treatment	Electrode	0.1	JTS K 0102-12.1
EC	No-pre-treatment	Conductivity meter	±5%	JTS K 0102-13
Na	No-pre-treatment	Flame photometry	0.02 mg/L	JTS K 0102-48.1
K	No-pre-treatment	Flame photometry	0.01 mg/L	JTS K 0102-49.1
Ca	Add 5ml of HCl (6mol/L) 500mL of sample	ICP-AES	0.01 mg/L	JTS K 0102-50.1
Mg	Add 5ml of HCl (6mol/L) 500mL of sample	ICP-AES	0.01 mg/L	JTS K 0102-51.1
Li	Add 5ml of HCl (6mol/L) 500mL of sample	ICP-AES	0.01 mg/L	----
Cl	No-pre-treatment	Ion chromatography	0.01 mg/L	JTS K 0102-35.3
SO_4	No-pre-treatment	Ion chromatography	0.1 mg/L	JTS K 0102-41.3
$T\text{-}CO_2$	Add 2ml of KOH (20wt%) 100mL of sample	Infrared analysis	5 mg/L	JTS K 0101-25.2
H_2S	Add 10mL of compound liquid of cadmium acetate (5wt%) and sodium acetate (3mol/L) per 500mL of sample	Iodometric method	0.5 mg/L	JTS K 0102-39.2
B	No-pre-treatment	ICP-AES	0.01 mg/L	JTS K 0102-47.3
SiO_2	Add 5ml of HCl (6mol/L) 500mL of sample	Gravimetric method	0.01 mg/L	JTS K 0101-44.3.2
T-Fe	Add 5ml of HCl (6mol/L) 500mL of sample	ICP-AES	0.01 mg/L	JTS K 0102-57.4
Al	Add 5ml of HCl (6mol/L) 500mL of sample	ICP-AES	0.01 mg/L	JTS K 0102-58.4
T-Hg	Add 5ml of HCl (6mol/L) 500mL of sample	AAS	0.005 mg/L	JTS K 0102-66.1.2
δD	No-pre-treatment	Mass spectrometry	±1% SMOW	JIkken Kagaku Koza
$\delta^{18}O$	No-pre-treatment	Mass spectrometry	±0.1%SMOW	JIkken Kagaku Koza
Fumarolic Gas Samples				
H_2O	---	Volume measurement	---	---
H_2S	Absorb into KOH aqueous solution (5mol/L), Then fix CdS by adding 10 mL cadmium acetate (5 wt%)	Iodometric method	0.5 mg/L	JIS K 0102-39.2.2
CO_2	Absorb into KOH aqueous solution (5mol/L)	Infrared method	5 mg/L	JIS K 0101-25.2
H_2	---	Gas chromatography	---	JIS K 2301
N_2	---	Gas chromatography	---	JIS K 2301
CH_4	---	Gas chromatography	---	JIS K 2301
He	---	Gas chromatography	---	JIS K 2301
Ar	---	Gas chromatography	---	JIS K 2301

O_2	---	Gas chromatography	---	JIS K 2301
$^3He/^4He$	---	Mass spectrometry	Depends	New- JIkken Kagaku Koza
$^4He/^{20}Ne$	---	Mass spectrometry	±10%	New- JIkken Kagaku Koza
$\delta^{13}C$	Absorb into KOH aqueous solution (5mol/L)	Mass spectrometry	±0.2% PDB	JIkken Kagaku Koza

3. GEOTHERMOMETERS

Chemical and isotope geothermometers constitute the most important geochemical tool for exploration and development of geothermal resources. When applying these geothermometers, it is assumed that no changes in water composition occur in conjunction with conductive cooling; boiling is taken to be adiabatic (D'Amore and Arnórsson, 2000). These methods were applied to give information on the source of geothermal fluid and an estimation of temperature conditions in the geothermal reservoir.

3.1 Solute Geothermometers

The most commonly used geothermometers for aqueous solutions are the silica (SiO_2) geothermometers that are based on the solubility of silica minerals, such as quartz or chalcedony. The quartz geothermometer is generally applicable at temperatures above 180°C and even at lower temperatures in systems where quartz is present in the host rock. For higher temperatures, the content of silica is generally controlled by quartz (Arnórsson, 1975). The formulae are given in Table 3, including the chalcedony geothermometer of Fournier (1977) and the quartz geothermometers for boiled and unboiled solutions published by Fournier and Potter (1982).

The Na/K geothermometers are for thermal waters and use the concentration (or activity) ratio of Na to K in the solutions. If the aqueous solutions are in equilibrium with Na- and K-bearing aluminosilicates the ratio of Na^+ and K^+ is fixed at a given temperature. White (1965) and Ellis (1969, 1970) were the first to present the relationship between Na/K ratios and temperature.

3.2 Gas Geothermometers

Gas geothermometers are often used, during the exploration phase, to estimate deep temperatures. The gases most often employed are the major reactive geothermal gases: CO_2, H_2S, H_2 and CH4, and inert gases such as N_2 and Ar.

Table 2: Equations for solutes and gas geothermometers; *S* represents the concentration of SiO2 in mg/kg; *Y* represents the logarithm of molal concentration ratio of Na/K; X represents gas concentrations in mole per cent ;T is in Kelvin; *Na, K, Mg* and *Ca* represent the concentrations of these elements in mg/kg.

Component	**Temperature equation (°C)**	**Published by:**
SiO_2, chalcedony	$t = \frac{1309}{5.19 - logS}$	Fournier, 1977
SiO_2, quartz	$t=-42.2+0.28831S-3.6686\times10-4S2+3.1665\times10-7S3+77.034\log S$	Fournier and Potter, 1982
SiO2, quartz, boiled	$t=-53.5+0.11236S-0.5559\times10-4S2 + 0.1772\times10-7S3+88.390\log S$	Fournier and Potter, 1982
Na-K	$t=733.6-770.551Y+378.189Y2 - 95.753Y3+9.544Y4$	Arnórsson et al., 1998a
Na-K	$t = \frac{1390}{1.750+\log(\frac{Na}{K})} - 273.15$	Giggenbach, 1988
K-Mg	$t = \frac{4410}{14.0 + \log(\frac{K^2}{Mg})} - 273.15$	Giggenbach, 1988
Na-Ca	$t = \frac{1096.7}{3.08 - \log(\frac{Na}{\sqrt{Ca}})} - 273.15$	Tonani, 1980
T_{MC} (CH_4-CO_2)	$t=(4625/(10.4+\log(X_{CH4}/X_{CO2})))-273$	Giggenbach,1991
T_{HA} (H_2-Ar)	$t=70(2.5+\log(X_{H2}/X_{Ar})$	Giggenbach,1991
T_{CA} (CO_2-Ar)	$\log(CO2/Ar)=-0.04+0.0277T+2048T$	Giggenbach,1991

Table 3: Table results of chemical analysis for water samples.

	Type	Date	Temp °C	pH	EC µS/cm	SiO_2 mg/L	Cl mg/L	SO_4 mg/L	HCO_3 mg/L	F mg/L	Na mg/L	K mg/L	Ca mg/L	Mg mg/L	Al mg/L	Fe mg/L	B mg/L	As mg/L	δD %	$\delta^{18}O$ %
Dirdir	Water well	27/01/2016	28.8	7.5	4170	65	852	589	198	8.7	862	3.6	47	4.8	<0.01	0.02	2.7	0.02	-21	-2.5
Kori	Hot spring	28/01/2016	48.0	7.8	3780	131	1000	224	169	2.6	724	20	50	4.0	<0.01	<0.01	0.61	0.02	-5	-0.4
Kori	Hot spring	29/9/2016	53.8	8	1617	101	273	176	112	2.2	262	14	29	3.6	<0.01	<0.01	0.35	0.004	-1	0.0
Garabbayis	Steam condensate	29/01/2016	99.7	5.8	36	0.11	0.04	0.73	153	<0.01	<0.01	<0.01	<0.01	<0.01	<0.01	<0.01	0.01	<0.01	-51	-8.5

Table 4: Table results of chemical analysis for fumarolic samples.

Table 3: Table results of chemical analysis for water samples. Survey site		**Hanle**								
Sampling Point		**Dirdir**	**Adha'amo**	**Goros**	**Dimbil**	**Lafofili**	**Garabbayis north**	**Garabbayis**	**Garabbayis**	**Garabbayis**
Date		22/01/2016	23/01/2016	23/01/2016	24/012016	25/01/2016	26/01/2016	07/04/2015	07/04/2015	30/04/2014
Y		11,434015	11,446890	11,458625	11,458735	11.338409	11,41635704	11,40648055	11,407561	11,40648056
X		42,279480	42,185024	42,211182	42,235676	42.219727	42,174037933	42,180689	42,1802	42,180689
T air	(°C)	35.8	31,8	32,4	28.4	31.1	33.8	36.2	39.3	32.3
T fumarole	(°C)	113.8	98,5	102,1	97.1	108.8	100.9	98.6	98.8	99.8
Boiling point	(°C)	99.7	98.9	98,7	98.6	99.2	99.1	99.0	99.0	99.5
H_2O	(vol%)	0.00	0.00	99,98	0.00	0.00	0.00	97.17	99.98	99.98
NCG	(vol%)	100.0	100.0	0,02	100.00	100.0	100.0	2.83	0.02	0.02
H_2S	(vol%)	0.0	0.00	30.2	0.0	0.0	0.0	4.1	12.1	0.0
CO2	(vol%)	0.0	0,00	0,0	0.0	0.0	0.0	0.0	15.0	45.0
R gas	(vol%)	100.0	100.0	69.8	100.0	100.0	100.0	95.9	72.9	55.0
H2	(vol%)	0.0005	0.0006	2	0.004	0.0004	0.0010	0.002	0.063	0.054
N2	(vol%)	77.9	78.1	90.3	77.9	77.9	78.1	78.7	95.1	93.5
CH4	(vol%)	n.d	n.d	0.35	n.d	n.d	n.d	n.d	0.98	1.0
O2	(vol%)	21,1	21.0	5.5	21.2	21.2	21.0	20.4	2.0	3.6
He	(vol%)	0,0008	0.0006	0.0039	0.0005	0.0008	0.0006	0.0010	0.018	0.019
Ar	(vol%)	0,91	0.91	1.9	0.91	0.91	0.91	0.93	1.8	1.8
3He/4He	(×10-6)	3,91±0,05	1.42±0.03	6.13±0.05	1.57±0.03	1.57±0.04	1.57±0.04	---	---	7.13±0.06
4He/20He	(×10-6)	0.479	0.251	3.42	0.276	0.300	0.348	----	---	11.6

4. RESULTS AND DISCUSSION

The Results of the analysis for water samples are shown in Table 3. The hot spring of Kori is a slightly alkaline water measuring water temperature varying from 48.0°C (January) to 53.8°C (September). The chemical and isotopic composition also varied between January and September.

4.1 Cl-SO4-HCO3 Ternary Diagram

The ternary diagram shown in Figure 4 classifies geothermal waters using the major anion concentrations (chloride, sulfate and bicarbonate) (Giggenbach, 1988). It also helps with distinguishing the waters as mature, peripheral, volcanic or steam-heated.

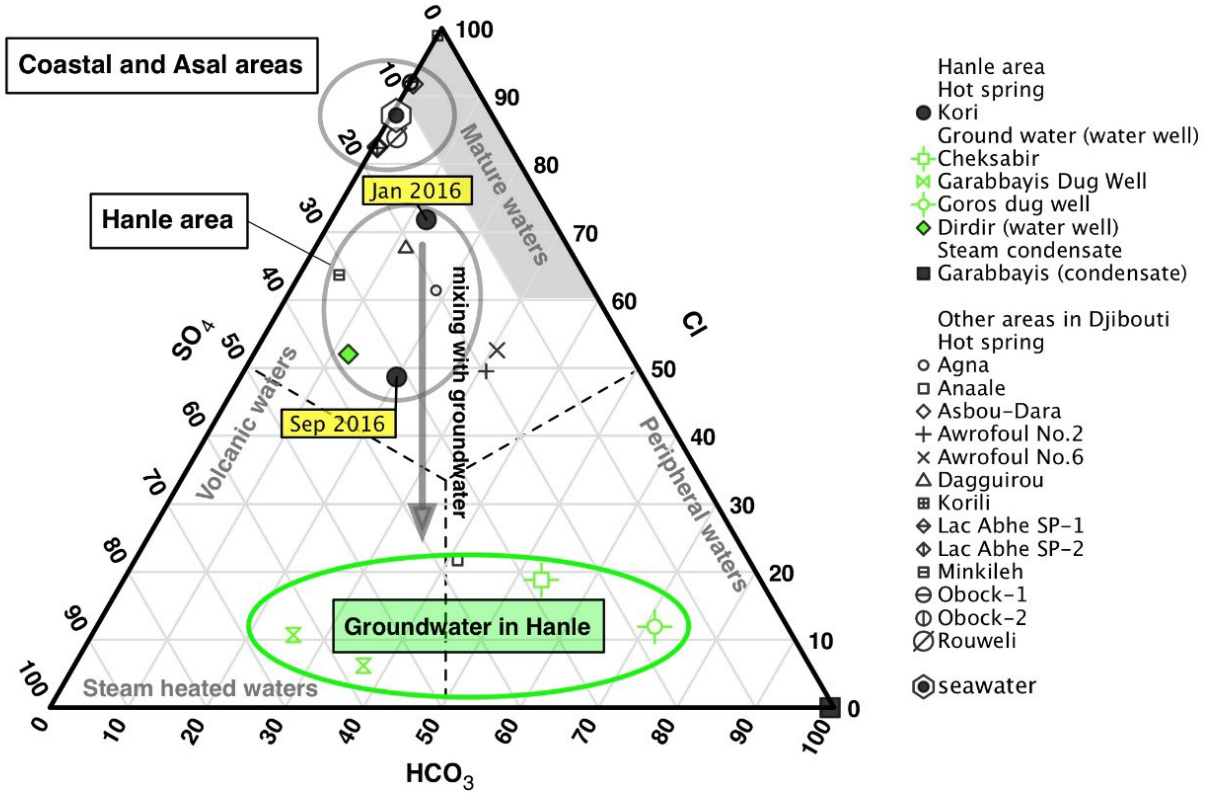

Figure 4: Relative Cl, SO4, and HCO3 contents of water samples.

Kori in January is similar to Agna, Dagguirou, and Minkileh in the Hanle plane, which show a relatively large content of Cl. Kori water appears to be created by mixing of fossil seawater and groundwater (HCO_3 water). It is also noted that the Cl content decreased in September compared to January, which can be explained by an increase in the mixing ratio of groundwater.

4.2 Na-K-Mg Ternary Diagram

The ternary diagram of Na-K-Mg was developed by Giggenbach (1988). It can be used to estimate the reservoir temperature and to select the waters most suitable for geothermometry.

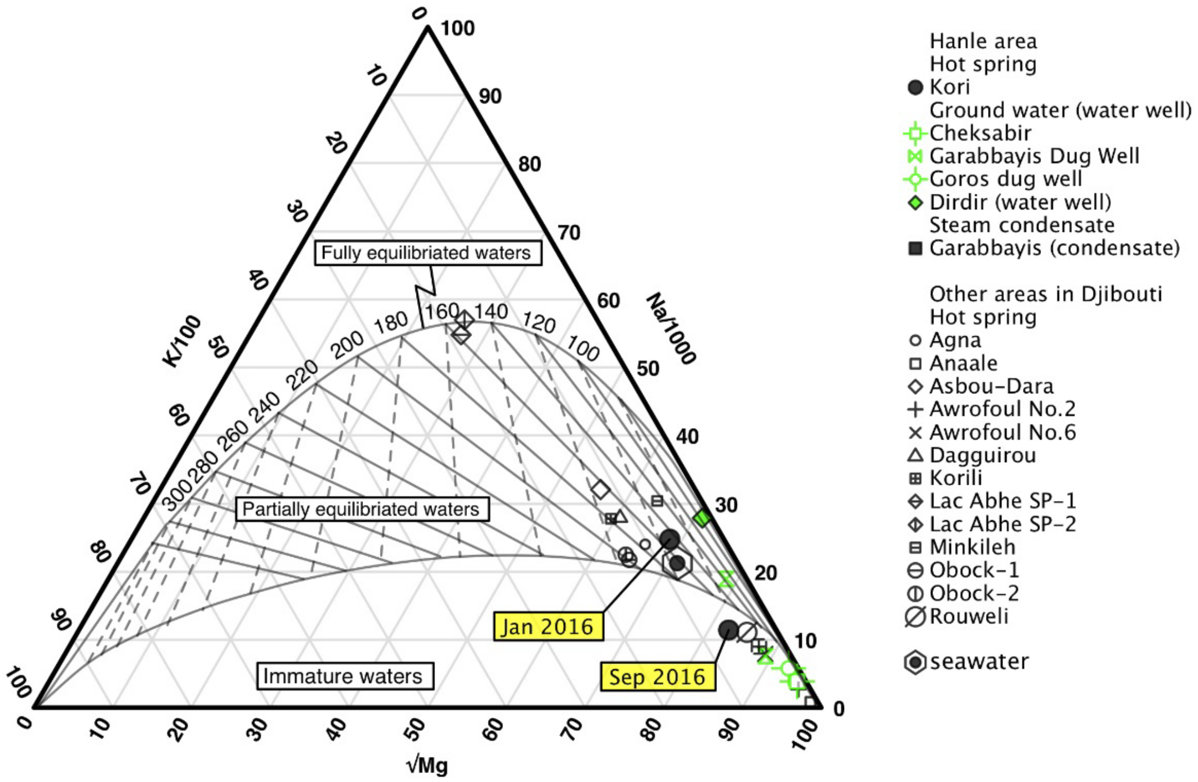

Figure 5: Relative K, Na, and Mg contents of water samples.

This diagram in Figure 5 indicates that the Kori hot spring in January is partially equilibrated with rock, which means that the Kori spring has temperature conditions under which water–rock interaction proceeds to some extent. In September, the Kori hot spring is plotted in immature waters out of the partial equilibrium. This is probably because that the Kori hot spring water was diluted more with groundwater in September than in January.

4.3 Silica and Cation Geothermometers of Kori

Results of calculation of geochemical thermometers using the chemical composition of the Kori hot spring are shown in Table 5. Because neutral, weak alteration of rock is observed in the Hanle area, chalcedony was selected as a major mineral that reacts with the spring water. A thermometer of chalcedony computes the reaction temperature at 125°C. This result suggests that the temperature of the hot spring aquifer, which is shallower than the geothermal reservoir, is about 125°C.

Table 5: Results of geochemical thermometers for the Kori hot spring.

Sample	Geothermometers (°C)						
	Quartz	Chalcedony	Na-k	Na-k	Na-k	K-Mg	Na-K-Ca
Kori	142	125	115	127	147	94	134
Kori	126	110	153	169	187	86	153

4.4 Origin of Water

As can be seen in Figure 6, the groundwater shows less relative content and a low concentration of Cl except for the Dirdir water well. In the figures, the plots of hot springs in the Hanle area roughly show a trend approaching the composition of the groundwater. In Figure 7, most of the samples are plotted on and close to a local meteoric water line except for the steam condensate.

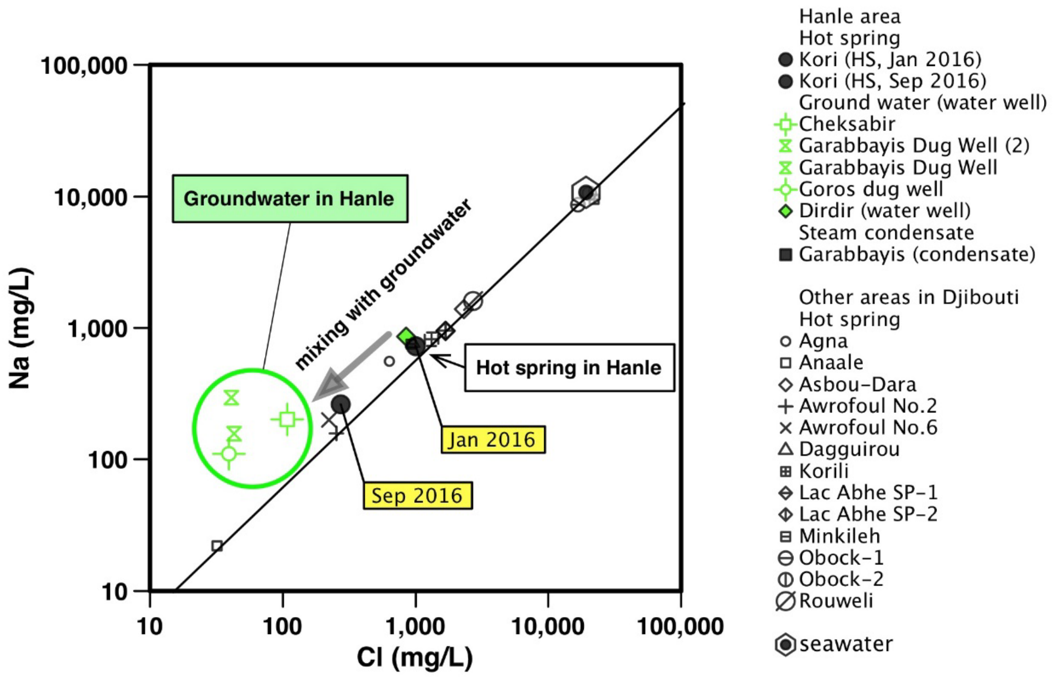

Figure 6: Relationship between Na and Cl for the water samples.

4.5 Gas

The results of the analysis for the fumarolic gas are shown in Table 4. Those fumarolic gas samples contain atmospheric soil gas in large concentrations. We added the results of gas sampling from previous survey performed in 2014 and 2015 at Garabbayis (JICA, 2014 and 2015). Most fumaroles in and around the Hanle lava plateau have low flow rates. On the other hand, the fumaroles at Goros and Garabbayis show relatively large flow rates, which means that they are located in the region where the flow of the ascending geothermal vapor is particularly vigorous.

4.5.1 Nature of Gas

Relative contents of He, Ar, and N_2 for fumarolic gases are shown in Figure 8. This diagram using analyzed raw data and corrected data for an air component, show that the fumaroles, except for Garabbayis and Goros, have a composition which is almost the same as that of the atmospheric (air) component.

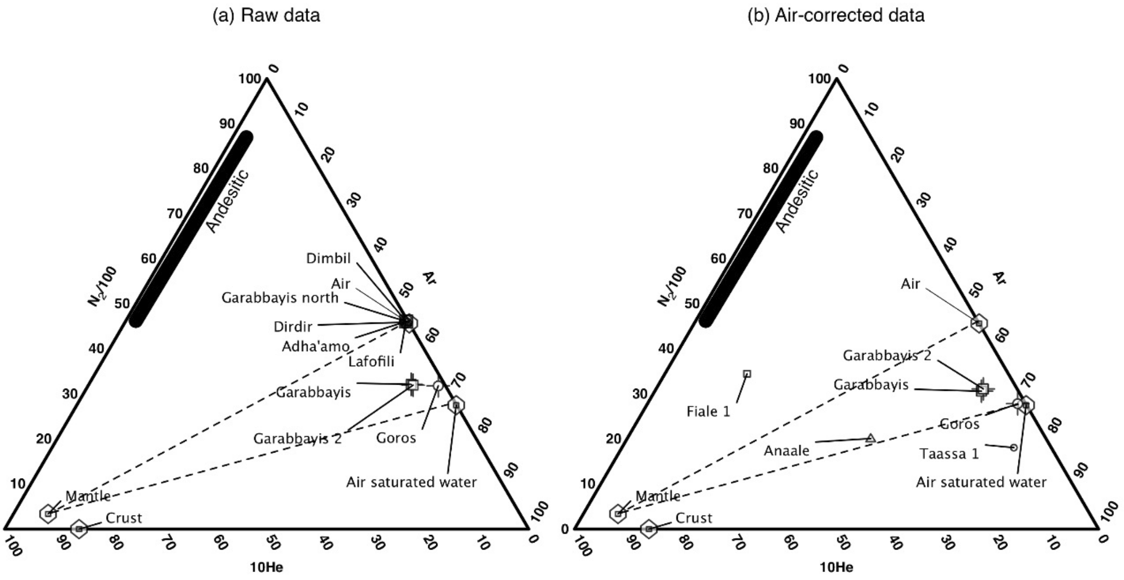
(a) Raw data

(b) Air-corrected data

Figure 8: Relative He, Ar, and N2 contents of fumarolic gases.

Figure 8 shows that Garabbayis and Goros contain a mantle component. A mantle component can be an indicator of the contribution of mantle or magma produced from the mantle to the geothermal system as the heat source.

4.5.2 Origin of Gas

In order to precisely examine the contribution of the mantle component, isotopic ratios of noble gases were analyzed. A correlation diagram of $^{3}He/^{4}He$ and $^{4}He/^{20}Ne$ is given in Figure 9. The fumaroles are plotted along the mixing curve of the atmospheric (air) and mantle components. The contribution of the mantle component is lower for Goros than for Garabbayis and is even lower for Dirdir.

In the case of Garabbayis, the contribution of the mantle component is visible in the relative contents of He, Ar and N_2, and in the isotopic ratios of noble gases (Figure 8). It can be said that the Garabbayis fumarole is fed with gas from the heat source.

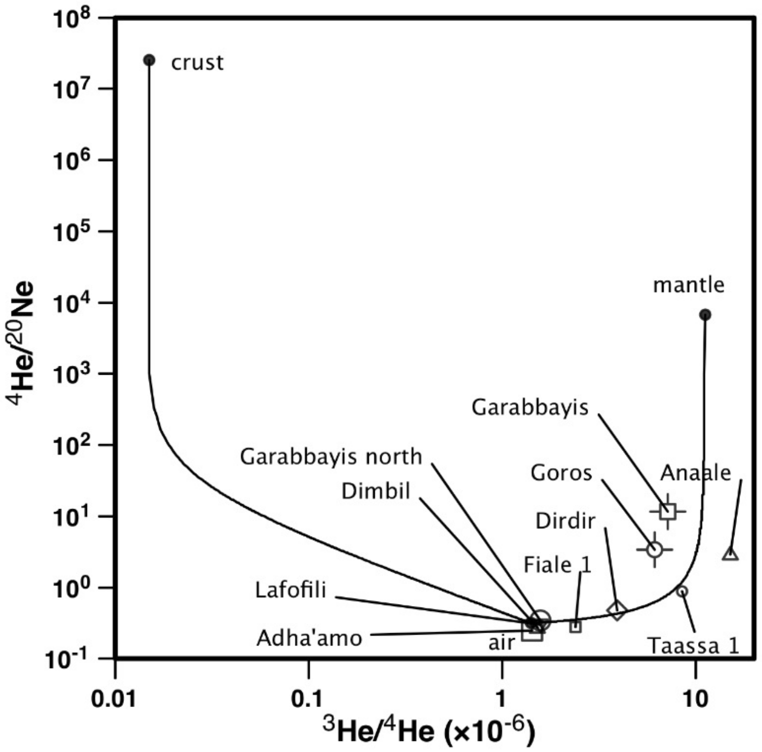

Figure 9: Relationship between 3He/4He and 4He/20Ne.

4.5.3 Gas Geothermomter

Gas geothermometers are often used, during the exploration phase, to estimate deep temperatures. Gas geothermometers have been formulated to estimate reservoir temperatures from gas concentrations in steam, assuming either gas-gas or gas-mineral equilibria at depth. The gases most often employed are the major reactive geothermal gases; CO_2, H_2S, H_2 and CH_4, sometimes in conjunction with inert gases such as N_2 and Ar. The main gas geothermometers applied in this report can be seen in Table 2.

Table 6: Results from gas geothermometers for Goros and Garabbayis.

	Goros	Garabbayis 1	Garabbayis 2
T_{HA}	179°C	74°C	72°C
T_{CA}	–	121°C	159°C
T_{MC}	–	234°C	266°C

Gas geothermometers which use ratios of H_2/Ar, CO_2/Ar, and CH_4/CO2 (Giggenbach, 1991), were applied to the gas composition of Goros and Garabbayis. In Table 6, the maximum temperatures are 179 °C (T_{HA}) and 266 °C (T_{MC}) for Goros and Garabbayis, respectively. As a result, the reservoir temperature is estimated to be 180°C–260 °C.

5. CONCLUSION

The origins of the hot spring water at Hanle seem to be from mixing of groundwater and fossil seawater or dissolution of evaporite by heated groundwater. Fumarolic gas is composed of mantle and atmospheric components. The detection of the mantle component and vapor water in steam at Garabbayis and Goros probably indicates a large flow rate of geothermal steam ascending from a depth to the surface.

Gas geothermometers suggest reservoir temperatures between 180°C and 260°C. While the solute geothermometer give an estimate of the temperature in an aquifer of hot springs at 125°C. We deduce that a geothermal reservoir sits under the central area of the Hanle lava plateau where geothermal steam seems to ascend with a large flow rate to the surface at Garabbayis and Goros.

REFERENCE

Arnórsson, S. (2000) The quartz and Na/K geothermometers. I. new thermodynamic calibration. Proceedings of the 2000 World Geothermal Congress, Kyushu-Tohoku, Japan, May 28-June 10, 929-934.

Ellis, A.J., 1969: Present-day hydrothermal systems and mineral deposition. Proceedings of the 9th Commonwealth Mining and Metal Congress, Inst. Min. Metall., London, 1-30.

Ellis, A.J., 1970: Quantitative interpretation of chemical characteristics of hydrothermal systems. Geothermics, 2, 516-527.

Fournier, R. O. (1979) Revised equation for the Na/K geothermometer. Transactions - Geothermal Resources Council, 3, 221-224.

Fournier, R. O. and Truesdell, A. H. (1973) An empirical Na-K-Ca geothermometer for natural waters. Geochimica et Cosmochimica Acta, 37, 1255 - 1275.

Fournier, R.O., and Potter, R.W. II, 1982: A revised and expanded silica (quartz) geothermometer. Geoth. Res. Council Bull.,11-10, 3-12.

Fournier, R.O., 1977: Chemical geothermometers and mixing model for geothermal systems. Geothermics, 5, 41-50.

Giggenbach, W. F. (1988) Geothermal solute equilibria. Derivation of Na-K-Mg-Ca geoindicators. Geochimica et Cosmochimica Acta, 52, 2749 - 2765.

Giggenbach, W. F. (1991) Chemical techniques in geothermal exploration. In D'Amore, F. (Eds.), Rome, UNITAR/UNDP Centre on Small Energy Resources, 119-144.

Fournier, R.O., 1977: Chemical geothermometers and mixing model for geothermal systems. Geothermics, 5, 41-50.

JICA (2014) Data collection survey on geothermal development in The Republic of Djibouti, Final Report.

JICA (2015) Data collection survey for geothermal development in The Republic of Djibouti (Geophysical survey), Final Report.

White, D.E., 1965: Saline waters of sedimentary rocks. Proceedings of the Symposium „Fluids in Subsurface Environments“. Amer. Assoc. Petrol. Geol., Mem., 4, 352-366.